Phylogeography of *Baryancistrus xanthellus* (Siluriformes: Loricariidae), a rheophilic catfish endemic to the Xingu River basin in eastern Amazonia

Keila Xavier Magalhães, Raimundo Darley Figueiredo da Silva, André Oliveira Sawakuchi, Alany Pedrosa Gonçalves, Grazielle Fernanda Evangelista Gomes, Janice Muriel-Cunha, Mark H. Sabaj, Leandro Melo de Sousa

Published: August 27, 2021 • https://doi.org/10.1371/journal.pone.0256677

Abstract

Baryancistrus xanthellus (Loricariidae) is an endemic fish species from the Xingu River basin with its life history in the shallow rapid waters flowing over bedrock substrates. In order to investigate the genetic diversity and demographic history of *B. xanthellus* we analyzed sequence data for one mitochondrial gene (Cyt b) and introns 1 and 5 of nuclear genes Prolactin (Prl) and Ribosomal Protein L3 (RPL3). The analyses contain 358 specimens of *B. xanthellus* from 39 localities distributed throughout its range. The number of genetically diverged groups was estimated using Bayesian inference on Cyt b haplotypes. Haplotype networks, AMOVA and pairwise fixation index was used to evaluate population structure and gene flow. Historical demography was inferred through neutrality tests and the Extended Bayesian Skyline Plot (EBSP) method. Five longitudinally distributed Cyt b haplogroups for *B. xanthellus* were identified in the Xingu River and its major tributaries, the Bacajá and Iriri. The demographic analysis suggests that rapids habitats have expanded in the Iriri and Lower Xingu rivers since 200 ka (thousand years) ago. This expansion is possibly related to an increase in water discharge as a consequence of higher rainfall across eastern Amazonia. Conversely, this climate shift also would have promoted zones of sediment trapping and reduction of rocky habitats in the Xingu River channel upstream of the Iriri River mouth. Populations of *B. xanthellus* showed strong genetic structure along the free-flowing river channels of the Xingu and its major tributaries, the Bacajá and Iriri. The recent impoundment of the Middle Xingu channel for the Belo Monte hydroelectric dam may isolate populations at the downstream limit of the species distribution. Therefore, future conservation plans must consider the genetic diversity of *B. xanthellus* throughout its range.

Citation: Magalhães KX, Silva RDFd, Sawakuchi AO, Gonçalves AP, Gomes GFE, Muriel-Cunha J, et al. (2021) Phylogeography of *Baryancistrus xanthellus* (Siluriformes: Loricariidae), a rheophilic catfish endemic to the Xingu River basin in eastern Amazonia. PLoS ONE 16(8): e0256677. https://doi.org/10.1371/journal.pone.0256677

Editor: Juan Marcos Mirande, Fundacion Miguel Lillo, ARGENTINA

Received: March 28, 2021; **Accepted:** August 12, 2021; **Published:** August 27, 2021

Data Availability: All relevant data are within the manuscript.

Funding: 1. KXM and APG received master and doctoral fellowship, Coordenação de Aperfeiçoamento de Pessoal de Nível Superior - Brasil (CAPES Finance Code 001). 2. AOS and LMS receive grants from CNPq (304727/2017-2 and 309815/2017–7 respectively). 3. AOS received FAPESP grants (2012/50260-6 and 2016/02656-9). 4. LMS received grant from CNPq (Edital Universal, proc. 486376/2013-3). 5. JM-C received a grant from FAPESPA/VALE (043/2011). 6. Research supported in part by iXingu Project (NSF DEB–1257813, MHS).

Competing interests: The authors have declared that no competing interests exist.

Introduction

Loricariidae (sucker-mouth armored catfishes) is easily the most diverse family of catfishes (Siluriformes) with approximately five [1] or six [2] subfamilies, 115 genera and over 1000 species widely distributed throughout the freshwaters of South and Central America [3, 4]. The largest loricariid subfamily, Hypostominae, contains about 45 genera and 491 species [3, 4]. Although species of Hypostominae are morphologically conserved, pigmentation patterns are often highly variable and have been used to distinguish numerous forms at and below the species level. Such variation is often geographically tied to a specific river basin, or sometimes longitudinal stretches within a river basin (e.g., [5]).

Large clearwater river systems draining shield terrains in the Amazon and Orinoco basins hold the highest diversity of Hypostominae. Such rivers have naturally transparent waters due to low suspended sediment loads [6, 7]. The three largest clearwater rivers in the Amazon Basin, the Tocantins, Xingu and Tapajós, respectively, support the largest faunas of Hypostominae (e.g., [8]). Those three basins largely drain the Brazilian Shield uplands. Only their downstream portions lie on the sedimentary terrains of the lowland Amazon, where each river's channel becomes naturally flooded and forms an estuary-like channel named as "fluvial ria" [9]. Among those three clearwater tributaries, the Xingu River stands out due to the extremely complex and unique channel morphology when flowing over the fractured bedrocks of the Brazilian Shield. Known as Volta Grande do Xingu, this broadly zig-zag sinuous stretch is divided into a network of bedrock channels with numerous rocky rapids [10, 11].

The genus *Baryancistrus* includes eight described species with three occurring in the Xingu Basin, the endemics *Baryancistrus chrysolomus* and *Baryancistrus xanthellus* and the more widely distributed *Baryancistrus niveatus*. *Baryancistrus xanthellus* is restricted to where the channels of the Xingu River and its major tributaries, the Iriri and Bacajá, flow over Precambrian igneous and metamorphic rocks [12] of the Brazilian Shield (Fig 1). Commonly known as golden-nugget pleco, this species is recognized by

having gold-colored spots on the body and conspicuous yellow bands along the distal margins of the caudal and dorsal fins [13]. Because of its attractive color pattern, this species is highly popular as an ornamental fish [14]. In certain parts of the Xingu Basin, local communities consume *B. xanthellus* due to its abundance and relatively large adult size (up to 300 mm SL).

Fig 1. Different color patterns present in *Baryancistrus xanthellus*.
Photographs of live specimens taken right after collection. Not all color morphs are represented in the figure.
https://doi.org/10.1371/journal.pone.0256677.g001

Baryancistrus xanthellus is usually found in rapids over rocky substrates that vary in composition and heterogeneity. Specimens have been collected at depths greater than 20 m in flows of moderate to strong velocity. Like most loricariids, *B. xanthellus* is a nocturnal fish and classified as detritivore, feeding mostly on algae and aufwuchs [13, 15].

It is observed a large variation in pigmentation between populations of *B. xanthellus* from distinct localities in the Xingu, Iriri and Bacajá rivers. Several colour patterns are distinguished based on the relative size, intensity and distribution of yellow spots and distal bands on dorsal and caudal fins (Fig 1).

This remarkable polychromatism within *B. xanthellus* may be influenced by local changes in environmental conditions. The role of environmental changes in the diversification of Amazonian biota is critical to understanding the origin of immense tropical biodiversity [16]. Most studies on the genetic diversity of Amazonian biota have focused on forest taxa (e.g., [17–20]) with relatively few studies targeting aquatic taxa (e.g., [21]). Studies of population genetics and phylogeography are needed to infer historical events and processes that account for the current-day distribution of lineages and partitioning of genetic diversity within species [22, 23]. Thus, the phylogeographic patterns of *B. xanthellus* are studied here and compared to climate changes that affected habitats of eastern Amazon rivers during the late Quaternary in order to shed light on the processes influencing the diversification of rheophilic fishes in the rapids of large clearwater rivers.

Furthermore, considering its endemicity, commercial value, and importance as a protein source, detailed studies are needed on the population genetics and phylogeography of *B. xanthellus*. Those data can help design proper management plans and effective conservation strategies for this species in the Xingu River and its tributaries. Such studies are further compelled by the recent construction of the Belo Monte Dam Complex in the middle Xingu River [10, 24, 25].

This study evaluates genetic differentiation within *B. xanthellus* based on one mitochondrial gene (Cyt b) and introns 1 and 5 of nuclear genes Prolactin (Prl) and Ribosomal Protein L3 (RPL3), respectively. The main goal of this work is to understand the phylogeography and population structure throughout most of the species' range in the Xingu River basin. Our results are used to infer underlying historical factors and to discuss the conservation of *B. xanthellus* with respect to hydrological and fluvial landscape changes imposed by the Belo Monte Dam Complex. Such changes include the loss of rocky rapids due to the flooding of the Xingu channel above the impoundment dam and the severe dewatering and suppression of the flood pulse below the dam.

Materials and methods

Fieldwork

Analyzed specimens were collected at 39 localities in the Xingu Basin, including 24 sites in the main channel from Vitória do Xingu to São Félix do Xingu upstream, 13 sites in the Iriri River, the largest Xingu tributary, and two sites in the Bacajá River, another major tributary that flows into Volta Grande stretch of the middle Xingu (Fig 2 and Table 1). No experimentation was conducted on live specimens. All material was collected in accordance with Brazilian law, under scientific collection licence (SISBIO 31089–1) and was in accordance with the precepts of the ethics committee for animal use in research "Comissão de Ética no Uso de Animais (CEUA)" of Universidade Federal do Pará (UFPA), protocol number 3032120919.

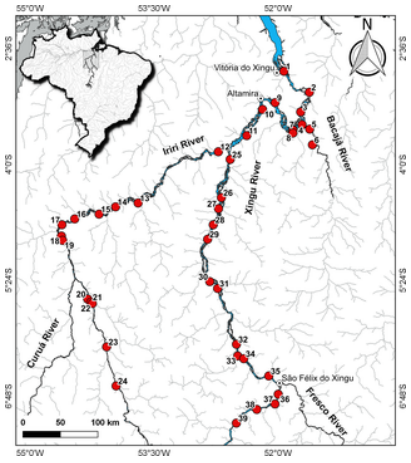

Fig 2. Map of collection sites of *Baryancistrus xanthellus* in the Xingu River basin; stretch of channel impounded by Belo Monte Dam (between site 8 and 10) not shown.
1: Vitória do Xingu; 2: Belo Monte; 3: Jericoá; 4: Percata; 5: Pariaxá; 6: Seca Farinha; 7: Ilha da Fazenda; 8: Igarapé Itatá; 9: Cotovelo; 10: Gorgulho da Rita; 11: Boa Esperança; 12: Cachoeira Grande; 13: Boa Esperança (Resex); 14: Cachoeira das Minhocas; 15: Ilha do Papagaio; 16: Cachoerinha; 17: Ressaca da Califórnia; 18: Lajeiro; 19: São Lucas; 20: Bené; 21: Pousada; 22: Porto Zé Carlos; 23: Zéfa; 24: Irineu; 25: Acima da confluência; 26: Balisa; 27: Pedra Preta (Resex); 28: Estragado; 29: Morro Grande; 30: Bela Vista; 31: Bom Jardim; 32: São Gonçalo; 33: Serra do Pardo; 34: Travessão do Nazaré; 35: Araraquara; 36: Remansinho; 37: Xadai; 38: Pedra Preta; 39: Onça.
https://doi.org/10.1371/journal.pone.0256677.g002

Locality		No. of individuals
1	Vitória do Xingu (XVX)	1
2	Belo Monte (XBM)	37
3	Jericoá (XJC)	22
4	Percata (BPT)	1
5	Pariaxá (BPX)	13
6	Seca Farinha (BSF)	10
7	Ilha da Fazenda (XIF)	30
8	Igarapé Itatá (XII)	4
9	Cotovelo (XCT)	23
10	Gorgulho da Rita (XGR)	8
11	Boa Esperança (XBE)	14
12	Cachoeira Grande (ICG)	25
13	Boa Esperança/Iriri (IBE)	1
14	Cachoeira das Minhocas (ICL)	4
15	Papagaio Island (IIP)	5
16	Cachoeirinha (ICA)	5
17	Ressaca da Califórnia (IRC)	1
18	Lajeiro (ILJ)	10
19	São Lucas (ISL)	4
20	Bené (IBN)	6
21	Pousada (IPD)	1
22	Porto Zé Carlos (IPC)	8
23	Zefá (IZF)	6
24	Irineu (IIU)	1
25	Acima da Confluência (XCC)	5
26	Balisa (XBL)	2
27	Pedra Preta/Resex (XRP)	8
28	Estragado (XED)	5
29	Morro Grande (XMG)	1
30	Bela Vista (XBV)	2
31	Bom Jardim (XBJ)	2
32	São Gonçalo (XSG)	5
33	Serra do Pardo (XSP)	5
34	Travessão do Nazaré (XTZ)	2
35	Araraquara (XAR)	16
36	Remansinho (XRE)	5
37	Xadai (XXA)	15
38	Pedra Preta (XPP)	15
39	Onça (XON)	30
	TOTAL	**358**

https://doi.org/10.1371/journal.pone.0256677.t001

Table 1. Number of individuals of *Baryancistrus xanthellus* sampled at each site.
Sites numbered according to the map in Fig 1; first letter of site abbreviation corresponds to river (i.e., “X” Xingu, “I” Iriri, “B” Bacajá).
https://doi.org/10.1371/journal.pone.0256677.t001

From 2012 to 2016, a total of 358 specimens of *B. xanthellus* were collected from throughout its range in the Xingu (n = 257), Iriri (77) and Bacajá (24) rivers. All specimen identifications were performed in the field and later confirmed using the original published description [13]. A small portion of muscle tissue or pelvic fin were removed from each individual and stored in cryogenic tubes of 96–99% ethanol. Voucher specimens were individually tagged, fixed in 10% formaldehyde, stored in ethanol 70% and cataloged into the zoological collections of the following institutions: Laboratório de Ictiologia de Altamira, Universidade Federal do Pará (LIA-UFPA), Brazil; Fish Collection of the Instituto Nacional de Pesquisas da Amazônia (INPA-ICT), Brazil, and The Academy of Natural Sciences of Philadelphia (ANSP), USA.

Labwork

Total DNA was isolated using the Wizard Genomic kit (Promega) according to manufacturer instructions. To access the quality of DNA, samples were run on a 1% agarose gel using a mixture of 2 μL of DNA and 2 μL of Gel Red™ (Biotium). After electrophoresis at 60 Volts for 30 minutes, DNA samples were visualized under ultraviolet light and photo-documented.

Three genomic regions were amplified via Polymerase Chain Reaction (PCR), including one mitochondrial gene, cytochrome b (Cyt b) and introns 1 and 5 of nuclear genes Prolactin (PRL) and Ribosomal Protein L3 (RPL3), respectively. Primers and annealing temperatures used for each marker are shown in Table 2.

Marker	Primers	Sequence (5'- 3')	Reference	Annealing (°C)
Cyt b	FishCytbF	ACCACCTTCGTATTCAACTACAAGAAC	[26]	55
	TrueCytbR	CCGACTTCGGGATTACAAGACCG		
RPL 3	RPL3SF	AAGAACTCCACCTATGCAGAT	[27]	54
	RPL3iR	TTCCGGGCAGTTTCTTTCTTTGCCA		
Prl	PrlSF	GCAAACTACACTCTCTCAGCCA	[28]	64
	PrlGR	TGRAGCGGAGAATCTCGCAC		

https://doi.org/10.1371/journal.pone.0256677.t002

Table 2. Primer sequences and PCR annealing temperatures used for each marker in the present study.
https://doi.org/10.1371/journal.pone.0256677.t002

PCR products were purified in PEG (Polyethylene Glycol) according to [29] and sequenced using the dideoxy-terminal method [30] with Big Dye kit reagents (ABI Prism^{TM} Dye Terminator Cycle Sequencing Reading Reaction) and an ABI 3500 automatic sequencer (Life Technologies, Foster City, CA, USA).

Data preparation

Sequences were manually edited in BioEdit [31] and aligned using the CLUSTALW method [32] available in that software. In the case of nuclear markers, the algorithm Phase v.2.0 [33] available in DNAsp v.5.10 [34] was applied to score the gametic phases of each individual. Five runs of PHASE consisted of 1,000 burn-in iterations and 1,000 principal iterations, with a thinning interval of 1. Output files from Phase were converted using the software SeqPhase [35]. Only haplotypes with probability values >0.6 were used in further analyses. Recombination events were estimated according to the pairwise homoplasy index (PHI) of [36] available in SplitsTree v.4.14.4 [37].

The number and frequency of haplotypes was evaluated in the software DNAsp v.5.10 [34], which was also used to prepare the input files for the software Arlequin [38].

Population and phylogeographic analyses

Descriptive parameters for each marker, such as number of polymorphic sites, and nucleotide (π) and haplotype (*h*) diversities, were established using the software Arlequin v.3.5.1.2 [38]. To verify the spatial and genealogic relationship of haplotypes for each marker, a haplotype network was built in the software Haploviewer [39] based on a Maximum Likelihood tree obtained in the PhyML package [40].

We applied the method implemented in BAPS 6 [41] to assign individuals to genetic clusters. With this method, the number of groups (i.e., genetically diverged lineages) is defined according to a Bayesian algorithm that estimates the distribution of allele frequencies in the tested populations [41]. Each analysis was performed 20 times for every level of K (1–20), with five replicates for each K. The K with the highest posterior probability (HPP) was chosen as the correct clustering.

Analysis of molecular variance (AMOVA) [42] was used to evaluate the genetic differentiation the population groups of *B*. *xanthellus* indicated by BAPS. AMOVA was carried out in Arlequin v.3.5.1.2 [38]. The significance level was calculated by conducting 10,000 permutations.

A geographic representation of the distribution and frequency of haplotypes was performed using the software GenGIS v2.2.0. [43].

To test for deviations from neutrality due to evolutionary processes within populations of *B*. *xanthellus*, the *Fs* [44] and *D* [45] values were estimated in Arlequin v.3.5.1.2 [38] based on 10,000 permutations.

Demographic history of *B*. *xanthellus* was inferred using the Extended Bayesian Skyline Plot (EBSP) method available in the software BEAST v.1.8 [46]. EBSP analysis was based on 100 million generations with genealogies sampled each 10,000 steps, according to the evolutionary model suggested by Kakusan v.4 [47] (i.e., HKY+G). A strict molecular clock was assumed based on a mutation rate of 0.76%/site/million of years within lineages, as suggested by Zardoya and Doadrio [48] for cytochrome b.

We checked convergence by visually inspecting and computing the effective sample size higher than 200) for each parameter in two independent runs using the program Tracer v.1.6 (available at http://beast.bio.ed.ac.uk/tracer), setting the burn-in to 10%. The remaining parameters and priors were used with the default values. EBSPs were plotted using R [49].

Results

Dataset and levels of genetic diversity

Sequence data for the 717-bp fragment of Cyt b revealed 169 polymorphic sites and 135 haplotypes among 358 individuals; 69% of those haplotypes were unique. BAPS analysis of the Cyt b fragment clustered individuals of *B*. *xanthellus* into five genetically diverged groups lettered A through E (Fig 1). The most frequent haplotype (H41) was shared by 69 individuals from Group C, followed by H4, shared by 19 individuals from Group A.

PHI tests assigned non-significant p-values to both introns, RPL3 (p = 0.9059) and Prl (p = 0.1623), indicating an absence of recombination events. For the RPL3 intron, 60 haplotypes were identified in a 225-bp fragment sequenced for 221 individuals. Haplotype H1 was shared by 123 individuals, followed by H4, present in 42 individuals. For the Prl intron, 203 haplotypes were found in a final fragment of 479 bp obtained from 224 individuals. The most frequent haplotypes for the Prl intron were H1 and H5, shared by 59 and 32 individuals, respectively (Table 3).

Population	N	Nh	S	h±dp	π±dp	Tajima (D)	Fu (Fs)
Cyt b							
A	71	26	28	0.891 +/- 0.025	0.0033 +/- 0.0020	-1.875*	-20.025**
B	21	12	14	0.910 +/- 0.048	0.0025 +/- 0.0016	-2.059**	-8.681**
C	139	57	67	0.806 +/- 0.033	0.0027 +/- 0.0017	-2.585**	-27.356**
D	92	37	45	0.944 +/- 0.012	0.0076 +/- 0.0041	-1.210	-18.205**
E	15	3	15	0.275 +/- 0.148	0.0030 +/- 0.0020	-2.235**	2.795
RPL3							
A	106	12	9	0.809 +/- 0.023	0.0061 +/- 0.0042	-0.513	-4.177*
B	42	8	7	0.453 +/- 0.094	0.0031 +/- 0.0027	-1.363*	-4.932*
C	162	25	17	0.799 +/- 0.026	0.0039 +/- 0.0041	-1.484*	-21.532**
D	132	11	6	0.244 +/- 0.052	0.0014 +/- 0.0016	-1.571*	-13.493**
E	10	4	4	0.533 +/- 0.180	0.0054 +/- 0.0043	-0.521	-0.439
PRL							
A	100	57	40	0.966 +/- 0.009	0.0071 +/- 0.0041	-1.791*	-26.219**
B	42	23	22	0.962 +/- 0.013	0.0075 +/- 0.0043	-0.986	-14.194**
C	170	84	34	0.971 +/- 0.006	0.0033 +/- 0.0032	-1.675*	-36.870**
D	124	31	18	0.930 +/- 0.010	0.0048 +/- 0.0030	-0.847	-23.352**
E	12	8	9	0.894 +/- 0.078	0.0060 +/- 0.0038	-0.218	-2.683

**p < 0.01.

*p < 0.05.

The sample number (N) for introns is duplicated due to heterozygosity.

https://doi.org/10.1371/journal.pone.0256677.t003

Table 3. Values of genetic diversity and neutrality *Fs* and D tests in *Baryancistrus xanthellus* based on the five genetically diverged groups (A–E) previously identified by BAPS analysis of Cyt b marker (N = number of individuals, Nh = number of haplotypes, S = polymorphic sites, h = haplotype diversity, and π = nucleotide diversity.

https://doi.org/10.1371/journal.pone.0256677.t003

For the five genetically diverged groups (A–E) inferred from the BAPS analysis, Cyt b haplotype diversity (*h*) ranged from 0.944 ± 0.012 (Group D) to 0.275 ± 0.148 (E) and nucleotide diversity (π) varied between 0.0023 ± 0.0016 (B) and 0.0076 ± 0.0041 (D). For the RPL3 nuclear intron, values of haplotype and nucleotide diversity ranged from *h* = 0.809 ± 0.023 (A) to 0.244 ± 0.052 (D) and π = 0.0061 ± 0.0042 (A) to 0.0014 ± 0.0016 (D). In the case of Prl nuclear intron, *h* values varied from 0.971 ± 0.006 (C) to 0.894 ± 0.078 (E) while π values ranged from 0.0075 ± 0.0043 (B) to 0.0048 ± 0.0030 (D) (Table 3).

Population genetic structure

Based on the mitochondrial marker (717-bp fragment of Cyt b), the BAPS analysis discriminated five genetically diverged groups within *B. xanthellus* (K = 5; logML = -3688.8922; Posterior Probability = 1) (Fig 3). Group A, named Resex of Iriri River, comprised 71 specimens from 12 sites along the Iriri and three sites in the Xingu channel, one immediately above and the first two sites downstream the Iriri-Xingu confluence. Group B (Resex of Xingu River) included 21 individuals from nine sites in the Xingu channel, all but one distributed from the first two sites downstream the Iriri-Xingu confluence upstream to about the midpoint between that confluence and São Felix do Xingu. Group C (Volta Grande do Xingu) included the largest number of individuals (159) and dominated the downstream-most limit of the species range, specifically the upper Xingu Ria, Middle Xingu channel downstream the mouth of the Iriri, and Bacajá River. Group D (São Félix do Xingu) comprised 92 individuals and dominated the upstream-most sites sampled in the Xingu channel. Group E (Ecological Station of Terra do Meio) included the fewest number of individuals (15) and was restricted to the upstream-most sites sampled in the Iriri River.

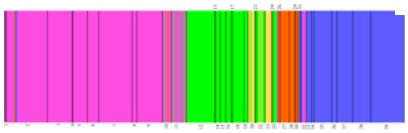

Fig 3. Estimation of genetically diverged groups in *Baryancistrus xanthellus* in the Xingu River basin inferred from the Bayesian analysis (BAPS) of 717-bp Cyt b fragment in 358 individuals.

The five groups are indicated by green (A), orange (B), magenta (C), blue (D) and yellow (E). The numbers represent the collection sites. 1: Vitória do Xingu; 2: Belo Monte; 3: Jericoá; 4: Percata; 5: Pariaxá; 6: Seca Farinha; 7: Ilha da Fazenda; 8: Igarapé Itatá; 9: Cotovelo; 10: Gorgulho da Rita; 11: Boa Esperança; 12: Cachoeira Grande; 13: Boa Esperança (Resex); 14: Cachoeira das Minhocas; 15: Ilha do Papagaio; 16: Cachoerinha; 17: Ressaca da Califórnia; 18: Lajeiro; 19: São Lucas; 20: Bené; 21: Pousada; 22: Porto Zé Carlos; 23: Zéfa; 24: Irineu; 25: Acima da confluência; 26: Balisa; 27: Pedra Preta (Resex); 28: Estragado; 29: Morro Grande; 30: Bela Vista; 31: Bom Jardim; 32: São Gonçalo; 33: Serra do Pardo; 34: Travessão do Nazaré; 35: Araraquara; 36: Remansinho; 37: Xadai; 38: Pedra Preta; 39: Onça.

https://doi.org/10.1371/journal.pone.0256677.g003

Genetically diverged groups B, C and D of *B. xanthellus* were restricted to the Xingu channel. Their frequency of occurrence formed a longitudinal gradient with the downstream range of the species dominated by Group B individuals, the middle portion dominated by Group C, and the upstream range, above São Felix do Xingu, exclusively Group D. Groups A and E were restricted to the Iriri channel except for a few Group A individuals found in the Xingu channel short distances upstream and downstream the mouth of the Iriri. Group E individuals had the smallest distribution and were limited to the furthest upstream sites in the Iriri River.

For Cyt b, the AMOVA (Table 4) showed that most of the genetic variation was found between the five genetically diverged groups (81.64%) instead of within groups (18.36%) (ϕST = 0.816). A different scenario was revealed from the analysis of nuclear regions. For both RPL3 and Prl introns, the AMOVA indicated that most of the variation is found within (90.38% and 87.86%, respectively) instead of among groups (Table 4).

Table 4. Analysis of Molecular Variance (AMOVA) to evaluate the genetic differentiation among and within the five genetically diverged groups of *B. xanthellus* indicated by BAPS.

https://doi.org/10.1371/journal.pone.0256677.t004

Substructure indices in populations of *B. xanthellus* from the Xingu River basin were corroborated by the allocation of Cyt b haplotypes to five clusters in the haplotype network. Group C comprised most of specimens from the region identified as Volta Grande do Xingu. The other groups discriminate the samples from São Félix do Xingu, Xingu Resex, Iriri Resex and the Ecological Station of Terra do Meio, revealing longitudinally structured populations along Xingu and Iriri rivers (Figs 4 and 5).

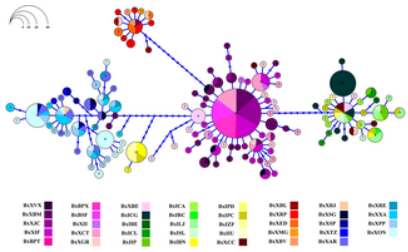

Fig 4. Haplotype network showing the distribution of 134 haplotypes in *Baryancistrus xanthellus* based on the mitochondrial Cyt b marker. Each color represents the 39 sampled sites in this study grouped accordingly: Iriri Resex (Group A–greenish), Xingu Resex (B–reddish), Volta Grande do Xingu (C–purplish), São Félix do Xingu (D–bluish), and Ecological Station of Terra do Meio (E–yellowish).
https://doi.org/10.1371/journal.pone.0256677.g004

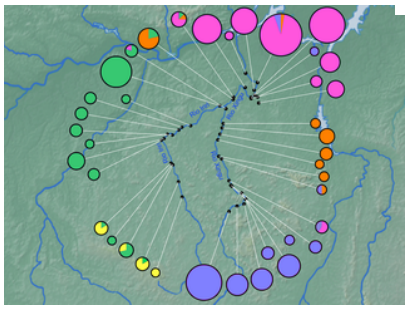

Fig 5. Distribution of Cyt b haplotypes of *Baryancistrus xanthellus* assigned to Group A (Iriri Resex–green), Group B (Xingu Resex–orange); Group C (Volta Grande do Xingu–magenta); Group D (São Félix do Xingu–blue), and Group E (Ecological Station of Terra do Meio–yellow).
https://doi.org/10.1371/journal.pone.0256677.g005

The lack of genetic substructure in nuclear markers was evident in the haplotype network, since no correlation was observed between haplotype and geographic distribution (Figs 6 and 7).

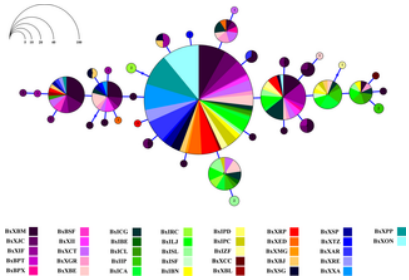

Fig 6. Haplotype network showing the distribution of 60 haplotypes in *Baryancistrus xanthellus* based on the nuclear RPL3 marker. Each color represents the 39 sampled sites in this study. The colors by group are: Iriri Resex (Group A–greenish), Xingu Resex (B–reddish), Volta Grande do Xingu (C–purplish), São Félix do Xingu (D–bluish), and Ecological Station of Terra do Meio (E–yellowish).
https://doi.org/10.1371/journal.pone.0256677.g006

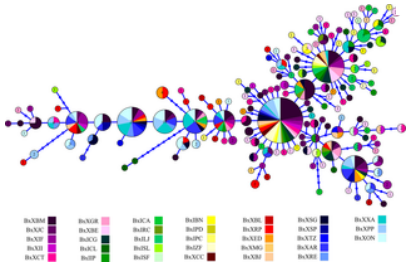

Fig 7. Haplotype network showing the distribution of 156 haplotypes in *Baryancistrus xanthellus* based on the nuclear PRL marker. Each color represents the sampled sites in this study. The colors by group are: Iriri Resex (Group A–greenish), Xingu Resex (B–reddish), Volta Grande do Xingu (C–purplish), São Félix do Xingu (D–bluish), and Ecological Station of Terra do Meio (E–yellowish).
https://doi.org/10.1371/journal.pone.0256677.g007

Demographic history

Negative and significant values were obtained in the *Fs* and *D* tests using both mitochondrial and nuclear markers for nearly all five population groups of *B*. *xanthellus*, indicating deviations from neutrality (Table 3).

The demographic history of each identified group (A–E) was inferred by Extended Bayesian Skyline Plots. The graphs obtained for groups A and C indicated a population expansion initiated 200 ka (thousand years ago). On the other hand, the effective population sizes (Ne) of groups B and D remained stable, while group E experienced a recent population expansion estimated at 5 ka (Fig 8).

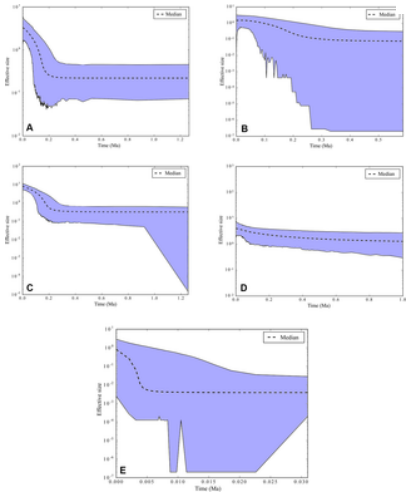

Fig 8. Bayesian Skyline Plot for the five lineages (Groups A–E) of *Baryancistrus xanthellus* from the Xingu River basin.
The curves correspond to the concatenated markers. The y axis corresponds to the effective population size (Ne) and the x axis corresponds to the mean period estimated in million years (Ma).
https://doi.org/10.1371/journal.pone.0256677.g008

Discussion

Genetic diversity, population structure and phylogeography

High levels of haplotype diversity (*h*) and low variation in nucleotide diversity (π) were observed in Cyt b sequences for three of the five groups analyzed: Iriri Resex (group A), Xingu Resex (B) and Volta Grande do Xingu (C). Reduced π values associated with high *h* values usually indicate bottleneck events followed by population expansion, thereby leading to accumulation of new mutations [50, 51]. A similar pattern suggestive of population expansion was reported in another species of Loricariidae, *Hypostomus ancistroides*, [52], as well as in other families of Siluriformes [53–55].

On the contrary, the group from São Félix do Xingu (group D) in the upper Xingu presented both high *h* and π values, typical of large and stable populations over long periods of evolutionary history [51]. For the group from the Ecological Station of Terra do Meio (group E) in the upper Iriri, both *h* and π diversity values were relatively low. This result might be explained by the reduced sample size of *B*. *xanthellus* from this region, as also inferred for some lineages of other Siluriformes, such as *Bagre bagre* (Ariidae) [56].

When compared to the other groups, the lowest haplotype diversity was detected in the groups from Volta Grande do Xingu at the downstream limit of the distribution of *B*. *xanthellus*. The Volta Grande do Xingu hosts the largest rapids and bedrock channels within the Xingu basin. This particular physiography may provide higher habitat availability and continuity for populations of *B*. *xanthellus*, favoring gene flow. Moreover, Volta Grande do Xingu supports most of colour morphs observed in *B*. *xanthellus*, making this stretch popular among ornamental fishermen over the last 40 years. Another commercially important loricariid species, *Hypancistrus zebra*, is endemic to Volta Grande and classified as Critically Endangered by the Brazilian Ministry of Environment [57] due to overfishing and habitat loss attributed to the Belo Monte dam complex. Accordingly, the group from this region also presented the highest number of shared haplotypes among individuals, suggesting the occurrence of population bottleneck.

The construction of the Belo Monte hydroelectric power plant, which began operations in the first quarter of 2016, might promote a spatial and temporal loss of genetic diversity in *B*. *xanthellus*. The population from Volta Grande do Xingu is directly affected by the loss of large rapids and availability of food resources due to sediment accumulation on rocky substrates in the reservoir and in the channel downstream of the impoundment dam [10, 11]. The change from lotic to lentic environments can cause drastic declines in populations of rheophilic and lithophilic fish species and eventually lead to local extinctions [24, 58].

The population structure inferred from Cyt b data revealed five haplogroups of *B*. *xanthellus* distributed along the Xingu River basin. These lineages were characterized by higher levels of intraspecific variation that indicate a strong population genetic substructure pattern.

In fact, the Xingu and Iriri rivers encompass high variety of aquatic environments, including powerful rapids with rocky substrates interspersed with backwaters with bottoms of sand or gravel [59]. Both rivers are often split into multiple channels with variable depths and levels of connectivity, the latter including steep drops that form waterfalls. This extreme variation in hydrodynamics and riverbeds promotes the fragmentation of aquatic habitats in the Xingu River, where rocky rapids are separated by slackwater stretches with substrates dominated by sediments.

Baryancistrus xanthellus is highly adapted to rocky rapids and, like most loricariid species, is phylopatric with no significant migration over breeding periods. These features might restrain gene flow among populations along a single bedrock river stretch [8]. Considering the longitudinal distribution of the five haplogroups herein identified, our observations of large backwater areas with deep channels and sediment-laden bottoms between rocky rapids might contribute to the limited dispersal of local populations. In other words, the isolation of shallow rocky rapids by large stretches of not so complex river channel with more calm waters leading to flow expansion and sediment accumulation combined with the biological particularities of *B. xanthellus* likely influenced genetic differentiation among populations of this species.

Nonetheless, some haplotyes of the Cyt b marker were shared between both neighboring and more distant populations. Putatively, this pattern points to a dynamic environment, wherein sediment accumulation and erosion would drive the fragmentation and expansion of rocky substrates. The sediment accumulation within rivers across space and through time depends on the interaction between channel morphology and water discharge. In the local scale, zones of channel widening and flow expansion are susceptible to sediment accumulation [60]. This would drive the distribution of riverbeds with exposed rocks or covered by sediments under a specific hydrological regime. Zones susceptible for sediment accumulation are also formed by the backwater effect of the trunk river in its tributaries. In this case, rocky riverbeds would be more fragmented or less persistent in the downstream reach of tributaries, difficulting the contact between populations of the trunk river (Xingu) and its tributaries (Iriri and Bacajá). In a thousand years timescale, periods of higher precipitation in eastern Amazonia increase the water discharge of the Xingu and Iriri rivers, favoring lateral or vertical channel erosion, sediment bypass and the expansion of zones of rocky rapids. This condition would promote some degree of gene flow among populations of *B. xanthellus*. On the other hand, dry periods would induce fluvial aggradation through accumulation of sediment within river channels [61], increasing the fragmentation of rocky rapids.

The rainfall in the Amazon region is driven by the South American monsoon system (SAMS) [62]. Eastern Amazonia, including the Xingu River basin, experienced remarkable variation in rainfall during the late Quaternary [63, 64]. For example, rainfall in eastern Amazonia was reduced during the last glacial maximum (~21–23 ka); conversely, rainfall may have increased during the middle Holocene (~6 ka) [64]. Abrupt climatic changes, such as the Heinrich Stadial 1 (HS1; ~18–15 ka), also promoted dramatic changes in rainfall and the water discharge of Amazonian rivers [65, 66].

Hydrology significantly impacts sediment transport and accumulation along river channels and consequently promotes changes in the continuity (or fragmentation) of rocky substrates. For eastern Amazonian rivers, periods of higher rainfall during the middle Holocene and HS1, would have increased the connectivity of fluvial channels and rocky rapids. On the other hand, the shift to a drier climate during last glacial maximum would have favoured the accumulation of sediments and the fragmentation of rocky rapids, isolating populations of species adapted to these habitats, such as *B. xanthellus*. Besides the climate variations reported since the last glacial maximum, the rainfall across Amazonia was modulated by insolation cycles with ~25 ka periodicity during the last 250 ka [63, 67]. These variations in hydrology and their effect on the sedimentary budget imply dynamic long-term distribution of rocky and sediment substrates of the Xingu River.

Similar patterns of population structure have been reported in other loricariid catfishes, such as *Hypostomus*. Based on the mitochondrial ATPase 6/8 marker, Hollanda et al. [52] identified 12 highly structured and genetically divergent populations of *H. ancistroides* from Paraná River basin. According to these authors, this pattern was related to the biological features of the species and to changes in environmental conditions. Also using ATPase 6/8 sequences, Borba et al. [68] performed phylogeographic and phylogenetic analyses on populations of *Hypostomus strigaticeps* from four sub-basins of the Paraná River. Their results confirmed that populations could be discriminated into two cryptic lineages within the single species.

Unlike those based on mtDNA, analyses based on nuclear markers often fail to detect subdivisions between populations, as was the case for *B. xanthellus*. Nuclear markers have lower rates of evolution when compared to mitochondrial markers, and are therefore less sensitive to recent events of population division [69].

Demographic history

Results obtained for nearly all samples by both *D* and *Fs* statistic tests suggest deviation of neutrality. Negative values may be interpreted as population expansion as suggested by the haplotype network star-like shape and by EBSP results [44]. In addition, the EBSP curves corroborated the neutrality tests, suggesting that population expansions in the A and C groups initiated about 200 ka. In contrast, the B and D groups seem remained stable over this period.

As previously discussed, rainfall in eastern Amazonia combined with channel hydrodynamics (zones of flow expansion and confluences) drives the capacity of clearwater rivers to trap (low rainfall) or transport (high rainfall) sediments to the Amazon River channel. Shield areas have very low rates of surface erosion [70], which point to relatively stable relief in the thousand years timescale. Thus, historical changes in rainfall and their consequent effect on fluvial sedimentation thereby have higher impact to the size and connectivity of rocky rapids during the late Quaternary.

Population expansion in groups A and C of *B. xanthellus* estimated over the last 200 Kya points to an increased availability of rocky rapids in the Iriri River and downstream stretch of the Xingu River. On the other hand, population stability in groups B and D suggests that aquatic environments in the Xingu River responded differently to regional climate changes, possibly due to hydrodynamic controls on the spatial distribution of sediment accumulation zones. These environmental dynamics in response to changes in rainfall could account for the high genetic diversity and population expansion or stability of *B. xanthellus* from different portions of the Xingu River basin. This hypothesis implies that similar phylogeographic patterns should be present in other loricariid catfishes sharing equivalent biological features and generation intervals.

Final remarks

This is the first study to characterize the phylogeographic pattern in *B. xanthellus* using mitochondrial and nuclear markers and encompassing a wide sampling over the entire species geographic range. Analyses of the Cyt b marker inferred five longitudinally distributed haplogroups with high genetic diversity in *B. xanthellus*. Those haplogroups are putatively associated with the philopatric nature of this species and the historical isolation of its preferred habitat (rocky rapids) driven by fluvial hydrodynamics and hydrological changes in eastern Amazonia over the late Quaternary. Analyses of the nuclear markers did not reveal a similar pattern due the recent nature of such diversification.

The demographic inferences indicated that some haplogroups have undergone population expansion while others have experienced population stability, both probably associated with spatial variation in aquatic habitats due to late Quaternary climate changes. Changes in water discharge driven by long-term changes in rainfall shifted the riverine landscape via sediment transport

or accumulation in the main channels. Consequently, rocky rapids have expanded (via sediment bypass) or retracted and fragmented (via sediment accumulation) along different stretches of the Xingu and Iriri Rivers during the last 200 ka.

Conservation strategies for *B. xanthellus* must take this phylogeographic pattern into account. The building and operation of the Belo Monte hydropower plant have significantly impacted the availability and connectivity of rocky rapids in the Volta Grande stretch of the Xingu channel and will likely reduce levels of genetic diversity and gene flow among resident populations. Furthermore, the ornamental fish trade of loricariids such as *B. xanthellus* should be monitored to avoid overfishing at sensitive localities.

Acknowledgments

We thank the curators and staff of the Laboratório de Ictiologia de Altamira, (UFPA/Altamira), Laboratório de Genética Aplicada, and Laboratório de Ictiologia e Biodiversidade Subterrânea (UFPA/IECOS-Bragança) for providing samples. Thanks to Marcella Santos and Mariangeles Arce for their important comments on earlier drafts of the manuscript. We thank Instituto Chico Mendes de Conservação da Biodiversidade (ICMBio), which through the ARPA consortium provided logistic and support for fieldwork.

References

1. Roxo FF, Ochoa LE, Sabaj MH, Lujan NK, Covain R, Silva GSC, et al. Phylogenomic reappraisal of the Neotropical catfish family Loricariidae (Teleostei: Siluriformes) using ultraconserved elements. Mol Phylogenet Evol. 2019;135: 148–165. pmid:30802595
View Article • PubMed/NCBI • Google Scholar

2. Pereira EHL, Reis RE. Morphology-based phylogeny of the suckermouth armored catfishes, with emphasis on the Neoplecostominae (Teleostei: Siluriformes: Loricariidae). Zootaxa. 2017;4264: 1. pmid:28609853
View Article • PubMed/NCBI • Google Scholar

3. Fricke R, Eschmeyer W, Fong JD. Species by Family/Subfamily. 2021. Available from:http://researcharchive.calacademy.org/research/ichthyology/catalog/SpeciesByFamily.asp
View Article • Google Scholar

4. Fricke R, Eschmeyer WN, Van Der Laan R. Eschmeyer's Catalog of Fishes: Genera, Species, References. 2021. Available from: http://researcharchive.calacademy.org/research/ichthyology/catalog/fishcatmain.asp.
View Article • Google Scholar

5. Camargo M, Ghilardi R. Entre a terra, as águas e os pescadores do médio rio Xingu: uma abordagem ecológica. Belém; 2009.
View Article • Google Scholar

6. Sioli H. The Amazon and its main affluents: Hydrography, morphology ofthe river courses. and river types. In: Sioli H. (ed.): The Amazon. Limnology and landscape ecology ofa mighty tropical river and its basin. 1984.
View Article • Google Scholar

7. Latrubesse EM, Stevaux JC, Sinha R. Tropical rivers. Geomorphology. 2005;70: 187–206.
View Article • Google Scholar

8. Camargo M, Junior HG, Sousa LM de, Py-Daniel LR. Loricariids of the Middle Rio Xingu. 2^{O}. Hannover: Panta Rhei; 2013.

9. Archer AW. Review of Amazonian Depositional Systems. Fluvial Sedimentology VII. Oxford, UK: Blackwell Publishing Ltd.; 2005. pp. 17–39.

10. Sabaj Pérez M. Where the Xingu Bends and Will Soon Break. Am Sci. 2015;103: 395.
View Article • Google Scholar

11. Sawakuchi AO, Hartmann GA, Sawakuchi HO, Pupim FN, Bertassoli DJ, Parra M, et al. The Volta Grande do Xingu: Reconstruction of past environments and forecasting of future scenarios of a unique Amazonian fluvial landscape. Sci Drill. 2015;20: 21–32.
View Article • Google Scholar

12. Neto Rocha. Programa Geologia do Brasil–PGB. Carta Geológica do Brasil ao Milionésimo. Folha Belém. 2004;A–22.

13. Py-Daniel LR, Zuanon J, de Oliveira RR. Two new ornamental loricariid catfishes of *Baryancistrus* from rio Xingu drainage (Siluriformes: Hypostominae). Neotrop Ichthyol. 2011;9: 241–252.
View Article • Google Scholar

14. Medeiros LA, Ginani EG, Sousa LM, Py-Daniel LHR, Feldberg E. Cytogenetic analysis of *Baryancistrus xanthellus* (Siluriformes: Loricariidae: Ancistrini), an ornamental fish endemic to the Xingu River, Brazil. Neotrop Ichthyol. 2016;14.
View Article • Google Scholar

15. Sampaio ZJA. História Natural da Ictiofauna de Corredeiras do rio Xingu, na região de Altamira, Pará. 1999. p. 199.
View Article • Google Scholar

16. Rull V. Neotropical biodiversity: timing and potential drivers. Trends Ecol Evol. 2011;26: 508–513. pmid:21703715
View Article • PubMed/NCBI • Google Scholar

17. Richardson JE. Rapid Diversification of a Species-Rich Genus of Neotropical Rain Forest Trees. Science (80-). 2001;293: 2242–2245. pmid:11567135
View Article • PubMed/NCBI • Google Scholar

18. Ribas CC, Aleixo A, Nogueira ACR, Miyaki CY, Cracraft J. A palaeobiogeographic model for biotic diversification within Amazonia over the past three million years. Proc R Soc B Biol Sci. 2012;279: 681–689. pmid:21795268
View Article • PubMed/NCBI • Google Scholar

19. Boubli JP, Ribas C, Lynch Alfaro JW, Alfaro ME, da Silva MNF, Pinho GM, et al. Spatial and temporal patterns of diversification on the Amazon: A test of the riverine hypothesis for all diurnal primates of Rio Negro and Rio Branco in Brazil. Mol Phylogenet Evol. 2015;82: 400–412. pmid:25285613
View Article • PubMed/NCBI • Google Scholar

20. Choueri ÉL, Gubili C, Borges SH, Thom G, Sawakuchi AO, Soares EAA, et al. Phylogeography and population dynamics of Antbirds (Thamnophilidae) from Amazonian fluvial islands. J Biogeogr. 2017;44: 2284–2294.
View Article • Google Scholar

21. Torati LS, Taggart JB, Varela ES, Araripe J, Wehner S, Migaud H. Genetic diversity and structure in Arapaima gigas populations from Amazon and Araguaia-Tocantins river basins. BMC Genet. 2019;20: 13. pmid:30691389
View Article • PubMed/NCBI • Google Scholar

22. Avise JC, Arnold J, Ball RM, Bermingham E, Lamb T, Neigel JE, et al. Intraspecific Phylogeography: The Mitochondrial DNA Bridge Between Population Genetics and Systematics. Annu Rev Ecol Syst. 1987;18: 489–522.
View Article • Google Scholar

23. Avise JC. Phylogeography: retrospect and prospect. J Biogeogr. 2009;36: 3–15.
View Article • Google Scholar

24. Lees AC, Peres CA, Fearnside PM, Schneider M, Zuanon JAS. Hydropower and the future of Amazonian biodiversity. Biodivers Conserv. 2016;25: 451–466.
View Article • Google Scholar

25. Winemiller KO, McIntyre PB, Castello L, Fluet-Chouinard E, Giarrizzo T, Nam S, et al. Balancing hydropower and biodiversity in the Amazon, Congo, and Mekong. Science (80-). 2016;351: 128–129.
View Article • Google Scholar

26. Sevilla RG, Diez A, Norén M, Mouchel O, Jérôme M, Verrez-Bagnis V, et al. Primers and polymerase chain reaction conditions for DNA barcoding teleost fish based on the mitochondrial cytochrome b and nuclear rhodopsin genes. Mol Ecol Notes. 2007;7: 730–734.
View Article • Google Scholar

27. Pinho C, Rocha S, Carvalho BM, Lopes S, Mourão S, Vallinoto M, et al. New primers for the amplification and sequencing of nuclear loci in a taxonomically wide set of reptiles and amphibians. Conserv Genet Resour. 2010;2: 181–185.
View Article • Google Scholar

28. Blel H, Panfili J, Guinand B, Berrebi P, Said K, Durand JD. Selection footprint at the first intron of the Prl gene in natural populations of the flathead mullet (Mugil cephalus, L. 1758). J Exp Mar Bio Ecol. 2010;387: 60–67.
View Article • Google Scholar

29. Paithankar KR, Prasad KS. Precipitation of DNA by polyethylene glycol and ethanol. Nucleic Acids Res. 1991;19: 1346. pmid:2030954
View Article • PubMed/NCBI • Google Scholar

30. Sanger F, Nicklen S, Coulson AR. DNA sequencing with chain-terminating inhibitors. Proc Natl Acad Sci U S A. 1977;74: 5463–5468. pmid:271968
View Article • PubMed/NCBI • Google Scholar

31. Hall T. BioEdit: a user-friendly biological sequence alignment editor and analysis program for Windows 95/98/NT. Nucleic Acids Symposium Series. 1999;41: 95–98.
View Article • Google Scholar

32. Thompson JD, Higgins DG, Gibson TJ. CLUSTAL W: Improving the sensitivity of progressive multiple sequence alignment through sequence weighting, position-specific gap penalties and weight matrix choice. Nucleic Acids Res. 1994;22: 4673–4680. pmid:7984417
View Article • PubMed/NCBI • Google Scholar

33. Stephens M, Donnelly P. Report A Comparison of Bayesian Methods for Haplotype Reconstruction from Population Genotype Data. Am J Hum Genet. 2003;73: 1162–1169. pmid:14574645
View Article • PubMed/NCBI • Google Scholar

34. Librado P, Rozas J. DnaSP v5: A software for comprehensive analysis of DNA poly- morphism data. Bioinformatics. 2009;25: 1451–1452. pmid:19346325
View Article • PubMed/NCBI • Google Scholar

35. Flot JF. Seqphase: A web tool for interconverting phase input/output files and fasta sequence alignments. Mol Ecol Resour. 2010;10: 162–166. pmid:21565002
View Article • PubMed/NCBI • Google Scholar

36. Bruen TC, Philippe H, Bryant D. A Simple and Robust Statistical Test for Detecting the Presence of Recombination. Genetics. 2006;172: 2665–2681. pmid:16489234
View Article • PubMed/NCBI • Google Scholar

37. Huson DH, Bryant D. Application of phylogenetic networks in evolutionary studies. Mol Biol Evol. 2006;23: 254–267. pmid:16221896
View Article • PubMed/NCBI • Google Scholar

38. Excoffier L, Lischer HEL. Arlequin suite ver 3.5: A new series of programs to perform population genetics analyses under Linux and Windows. Mol Ecol Resour. 2010;10: 564–567. pmid:21565059
View Article • PubMed/NCBI • Google Scholar

39. Salzburger W, Ewing GB, Von Haeseler A. The performance of phylogenetic algorithms in estimating haplotype genealogies with migration. Mol Ecol. 2011;20: 1952–1963. pmid:21457168
View Article • PubMed/NCBI • Google Scholar

40. Guindon S, Dufayard JF, Lefort V, Anisimova M, Hordijk W, Gascuel O. New algorithms and methods to estimate maximum-likelihood phylogenies: Assessing the performance of PhyML 3.0. Syst Biol. 2010;59: 307–321. pmid:20525638
View Article • PubMed/NCBI • Google Scholar

41. Corander J, Waldmann P, Sillanpää MJ. Bayesian analysis of genetic differentiation between populations. Genetics. 2003;163: 367–374. pmid:12586722
View Article • PubMed/NCBI • Google Scholar

42. Excoffier L, Smouse PE, Quattro JM. Analysis of molecular variance inferred from metric distances among DNA haplotypes: Application to human mitochondrial DNA restriction data. Genetics. 1992;131: 479–491. pmid:1644282
View Article • PubMed/NCBI • Google Scholar

43. Parks DH, Mankowski T, Zangooei S, Porter MS, Armanini DG, Baird DJ, et al. GenGIS 2: Geospatial Analysis of Traditional and Genetic Biodiversity, with New Gradient Algorithms and an Extensible Plugin Framework. Gilbert JA, editor. PLoS One. 2013;8: e69885. pmid:23922841
View Article • PubMed/NCBI • Google Scholar

44. Fu YX. Statistical tests of neutrality of mutations against population growth, hitchhiking and background selection. Genetics. 1997;147: 915–925. pmid:9335623
View Article • PubMed/NCBI • Google Scholar

45. Tajima F. Statistical method for testing the neutral mutation hypothesis by DNA polymorphism. Genetics. 1989;123: 585–595. pmid:2513255
View Article • PubMed/NCBI • Google Scholar

46. Drummond AJ, Rambaut A, Shapiro B, Pybus OG. Bayesian coalescent inference of past population dynamics from molecular sequences. Mol Biol Evol. 2005;22: 1185–1192. pmid:15703244
View Article • PubMed/NCBI • Google Scholar

47. Tanabe AS. Kakusan: a computer program to automate the selection of a nucleotide substitution model and the configuration of a mixed model on multilocus data. Mol Ecol Notes. 2007;7: 962–964.
View Article • Google Scholar

48. Zardoya R, Doadrio I. Molecular evidence on the evolutionary and biogeographical patterns of European cyprinids. J Mol Evol. 1999;49: 227–237. pmid:10441674
View Article • PubMed/NCBI • Google Scholar

49. R Core Team. R: A language and environment for statistical computing. R Foundation for Statistical. 2020; 2020.

50. Avise JC. Phylogeography: The History and Formation of Species. Cambridge M, editor. Harvard University Press; 2000.

51. Grant WS, Bowen BW. Shallow Population Histories in Deep Evolutionary Lineages of Marine Fishes: Insights From Sardines and Anchovies and Lessons for Coservation. J Hered. 1998;89: 415–426.
View Article • Google Scholar

52. Hollanda PC, Lima SMQ, Zawadzki HC, Oliveira C, de Pinna M. Phylogeographic patterns in suckermouth catfish *Hypostomus ancistroides* (Loricariidae): dispersion, vicariance and species complexity across a Neotropical biogeographic region. Mitochondrial DNA Part A. 2016;27: 3590–3596.
View Article • Google Scholar

53. Vergara J, Azpelicueta MDLM, Garcia G. Phylogeography of the Neotropical catfish *Pimelodus albicans* (Siluriformes: Pimelodidae) from río de la Plata basin, South America, and conservation remarks. Neotrop Ichthyol. 2008;6: 75–85.
View Article • Google Scholar

54. Bignotto T, Prioli A, Prioli S, Maniglia T, Boni T, Lucio L, et al. Genetic divergence between *Pseudoplatystoma corruscans* and *Pseudoplatystoma reticulatum* (Siluriformes: Pimelodidae) in the Paraná River Basin. Brazilian J Biol. 2009;69: 681–689. pmid:19738974
View Article • PubMed/NCBI • Google Scholar

55. Kumari P, Pavan-Kumar A, Kumar G, Alam A, Parhi J, Gireesh-Babu P, et al. Genetic diversity and demographic history of the giant river catfish *Sperata seenghala* inferred from mitochondrial DNA markers. Mitochondrial DNA Part A. 2016;0: 1–7. pmid:27608325
View Article • PubMed/NCBI • Google Scholar

56. Silva WC da, Marceniuk AP, Sales JBL, Araripe J. Early Pleistocene lineages of *Bagre bagre* (Linnaeus, 1766) (Siluriformes: Ariidae), from the Atlantic coast of South America, with insights into the demography and biogeography of the species. Neotrop Ichthyol. 2016;14: e150184.
View Article • Google Scholar

57. ICMBio. Instituto Chico Mendes de Conservação da Biodiversidade. Livro Vermelho da Fauna Brasileira Ameaçada de Extinção. 2018. Available: https://www.icmbio.gov.br/portal/images/stories/comunicacao/publicacoes/publicacoes-diversas/livro_vermelho_2018_vol1.pdf

58. Reis RE. Conserving the freshwater fishes of South America. Int Zoo Yearb. 2013;47: 65–70.
View Article • Google Scholar

59. Isaac V, Almeida MC, Cruz REA. and Nunes Lg. Artisanal fisheries of the Xingu River basin in Brazilian Amazon. Brazilian J Biol. 2015;75: 125–137. pmid:26691085
View Article • PubMed/NCBI • Google Scholar

60. North CP, Davidson SK. Unconfined alluvial flow processes: Recognition and interpretation of their deposits, and the significance for palaeogeographic reconstruction. Earth-Science Rev. 2012;111: 199–223.
View Article • Google Scholar

61. Paola C. Quantitative models of sedimentary basin filling. Sedimentology. 2000;47: 121–178.
View Article • Google Scholar

62. Zhou J, Lau KM. Does a Monsoon Climate Exist over South America? J Clim. 1998;11: 1020–1040.
View Article • Google Scholar

63. Cheng H, Sinha A, Cruz FW, Wang X, Edwards RL, D'Horta FM, et al. Climate change patterns in Amazonia and biodiversity. Nat Commun. 2013;4: 1411. pmid:23361002
View Article • PubMed/NCBI • Google Scholar

64. Wang X, Edwards RL, Auler AS, Cheng H, Kong X, Wang Y, et al. Hydroclimate changes across the Amazon lowlands over the past 45,000 years. Nature. 2017;541: 204–207. pmid:28079075
View Article • PubMed/NCBI • Google Scholar

65. Zhang Y, Chiessi CM, Mulitza S, Sawakuchi AO, Häggi C, Zabel M, et al. Different precipitation patterns across tropical South America during Heinrich and Dansgaard-Oeschger stadials. Quat Sci Rev. 2017;177: 1–9.
View Article • Google Scholar

66. Crivellari S, Chiessi CM, Kuhnert H, Häggi C, Portilho-Ramos RC, Zeng J-Y, et al. Increased Amazon freshwater discharge during late Heinrich Stadial 1. Quat Sci Rev. 2018;181: 144–155.
View Article • Google Scholar

67. Govin A, Chiessi CM, Zabel M, Sawakuchi AO, Heslop D, Hörner T, et al. Terrigenous input off northern South America driven by changes in Amazonian climate and the North Brazil Current retroflection during the last 250 ka. Clim Past. 2014;10: 843–862.
View Article • Google Scholar

68. de Borba RS, Zawadzki CH, Oliveira C, Perdices A, Parise-Maltempi PP, Alves AL. Phylogeography of *Hypostomus strigaticeps* (Siluriformes: Loricariidae) inferred by mitochondrial DNA reveals its distribution in the upper Paraná River basin. Neotrop Ichthyol. 2013;11: 111–116.
View Article • Google Scholar

69. Zink RM, Barrowclough GF. Mitochondrial DNA under siege in avian phylogeography. Mol Ecol. 2008;17: 2107–2121. pmid:18397219
View Article • PubMed/NCBI • Google Scholar

70. Wittmann H, von Blanckenburg F, Maurice L, Guyot J-L, Filizola N, Kubik PW. Sediment production and delivery in the Amazon River basin quantified by in situ-produced cosmogenic nuclides and recent river loads. Geol Soc Am Bull. 2011;123: 934–950.
View Article • Google Scholar